

Facile Preparation of Layered Ni(OH)₂/Graphene Composite from Expanded Graphite

Renjie Qu^{1,2,#}, Zhen Dai^{1,3,#}, Shuihua Tang^{1,2,*}, Zhentao Zhu^{1,2} and Geir Martin Haarberg^{4,*}

¹ State Key Lab of Oil and Gas Reservoir Geology & Exploitation, Southwest Petroleum University, Chengdu 610500, China.

² School of Materials Science and Engineering, Southwest Petroleum University, Chengdu 610500, P R China

³ School of Chemistry and Chemical Engineering, Southwest Petroleum University, Chengdu 610500, P R China

⁴ Department of Materials Science and Engineering, Norwegian University of Science and Technology, Trondheim 7491, Norway.

#: with identical contributions

*E-mail: spraytang@hotmail.com, geir.martin.haarberg@ntnu.no

Received: 30 June 2017 / Accepted: 11 August 2017 / Published: 12 September 2017

A layered Ni(OH)₂/graphene composite was firstly prepared by electrochemical deposition of nickel nanoparticles between layers of expanded graphite in Ni²⁺ containing solution, and then the deposited nickel nanoparticles were converted into Ni(OH)₂ via cyclic voltammetry in 6 M KOH electrolyte. Images of transmission electron microscopy show that Ni(OH)₂ particles are uniformly distributed on graphene sheets with an average diameter of 6 nm. The Ni(OH)₂/graphene composite with an areal loading of 5 mg cm⁻² demonstrates a maximum specific capacitance of 856 F g⁻¹ at 1 A g⁻¹, and 79 % of the specific capacitance can be retained after 2000 cycles at a current density of 10 A g⁻¹. Commercial expanded graphite is much cheaper than activated carbon and considerably much cheaper than graphene, therefore this technique is very promising for mass production of supercapacitor electrodes.

Keywords: Expanded graphite; Layered Ni(OH)₂/graphene; Electrodeposition; Supercapacitors; Nickel nanoparticle

1. INTRODUCTION

An electrochemical capacitor (EC) possesses advantages of high power density, long cycling life, friendly environment, and wide operation temperature window. Currently, commercialised EC

based on carbon materials confronts two big issues of high cost and low energy density, leads to its supporting role in electric vehicles, where it mostly supplies peak power and recovers power from braking energy. The next generation of EC is expected to come close to Li-ion battery in energy density while maintaining its high power density, so that EC can be used as a sole power source for automobiles.[1]

Pseudocapacitive materials such as conducting polymers and metal oxides/hydroxides usually have enhanced specific capacitance and energy density. However, conducting polymers have inherent drawbacks of swelling and unstable structures, [2] and metal oxides/hydroxides are also subjected to poor conductivity, large particle size and particle aggregation during a charging-discharging process. Therefore, combining both double-layer and pseudo-capacitance materials to synthesize composites is a good solution.

In recent years, tremendous research efforts have been attempted to design excellent performance composites through incorporating carbon materials with conducting polymers and/or transition-metal oxides/hydroxides. Among available transition-metal oxides/hydroxides, NiO/Ni(OH)₂ is attractive due to its high theoretical specific capacitance, low toxicity and cost.[3-5] Therefore, NiO or Ni(OH)₂/carbon material composite has been intensively explored.[6-14] Graphene has been regarded as an ideal EDLC electrode material owing to its high specific surface area and good electrical conductivity.[15, 16] But it is very expensive and has a tendency to stack back to graphite. Thus, Ni(OH)₂/graphene composite is intensively investigated to exert respective advantages and overcome each disadvantages in recent years.

Zhang *et al*[17] firstly mixed graphite oxide with hexamethylenetetramine and placed the mixture in a water bath for 14 h at 363 K. Nickel nitrate hexahydrate and hydrazine hydrate were added in and the mixture was reacted at 363 K for 2 h to obtain Ni(OH)₂/reduced graphite oxide (rGO) composite. A specific capacitance of 1008 F g⁻¹ was obtained at high current density of 42 A g⁻¹. Dubal *et al*[18] synthesized Ni(OH)₂/rGO by a chemical precipitation method, the reaction lasted 4 h at 343 K. The symmetric device assembled with as-prepared Ni(OH)₂/rGO composite demonstrated a specific capacitance of 812 F g⁻¹ with mass loading of 4.2 mg cm⁻² at 5 mV s⁻¹. Min *et al*[19] prepared rGO/Ni(OH)₂ films *via* one-pot hydrothermal synthesis, the corresponding reaction time and temperature were 24 h and 473 K, respectively. The results obtained by galvanostatic charge-discharge test indicated that the composite exhibited a high specific capacitance of 1667 F g⁻¹ at 3.3 A g⁻¹.

From above, we can see that time-consuming procedures and relatively high operating temperatures are often associated with chemical precipitation and hydrothermal process. Comparatively, electrochemical preparation of Ni(OH)₂/graphene usually can be conducted under ambient environment and is a time-saving process. Wang *et al*[20] prepared Ni(OH)₂ nanoflakes/graphene by electrochemical deposition. The composites exhibited high specific capacitance of 2161 F g⁻¹ at 3 A g⁻¹, and remained high at 1520 F g⁻¹ even when the current density was as high as 60 A g⁻¹. After 500 cycles, Ni(OH)₂ nanoflakes/graphene delivered a specific capacitance of 819 F g⁻¹ at a current density of 60 A g⁻¹. Yang *et al*[21] also prepared Ni(OH)₂/rGO by a two-step electrochemical process including electro-oxidation and electro-reduction. The Ni(OH)₂/rGO composites showed a specific capacitance of 1700 F g⁻¹ at 5 A g⁻¹ and 967 F g⁻¹ at 20 A

g^{-1} . Meanwhile, the electrode exhibited a specific capacitance of 950 F g^{-1} at a charge and discharge current density of 5 A g^{-1} after 500 cycle test.

From above, we can see all the $\text{Ni(OH)}_2/\text{graphene}$ composites showed excellent electrochemical performances. However, all of the studies were carried out directly on graphitic oxide (GO) or graphene. It is well known that preparation of GO or graphene is time-consuming and still in a lab-scale, thus it will lead to high cost and unrepeatable batches.

However, expanded graphite (EG), as a graphene-like 2D material, has been investigated in many fields, and it is a commercial product with illegible cost as compared to graphene (G). In this work, we address a route to use EG as a starting carbon material and Ni^{2+} ions containing solution as an electrolyte. Then the electrochemical deposition is carried out under certain conditions to assure that Ni nanoparticles are deposited between interlayer planes of graphite sheets except for the edges, and thus a layered Ni nanoparticles/graphene composite is obtained. Followed by activation of Ni/graphene in KOH solution via cyclic voltammetry (CV) before electrochemical test, a layered $\text{Ni(OH)}_2/\text{G}$ composite is finally synthesized. This procedure is facile, cost effective, environmentally friendly, and easily scaled-up, and may suitable for commercialized production.

2. EXPERIMENTAL

2.1 Materials

Expanded graphite (EG, Qingdao Jinrilai Graphite Company) was used as a carbon support, Nafion (5 wt%, Shanghai Hesen Electric Company) was applied as a binder, nickel foam (NF, 110 PPI, 320 g m^{-2} , Changsha Liyuan New Material Company) was mainly used as a current collector, nickel chloride hexahydrate ($\text{NiCl}_2 \cdot 6\text{H}_2\text{O}$, AR, Chendu Kelong Chemical Company) was utilized as a nickel source, potassium hydroxide (KOH, AR, Chendu Kelong Chemical Company) solution was applied as an electrolyte.

2.2 Synthesis of $\text{Ni(OH)}_2/\text{G}$ composites

EG and 5 wt% Nafion[®] solution with a dry mass ratio of 90:10 were ultrasonically dispersed in ethanol till homogeneous slurry was obtained, and then a dimension of 10×10 NF was dipped into the EG slurry, repeated several times while controlling the EG loading at 2 mg cm^{-2} . The as-prepared EG/NF electrode was applied as working electrode, a dimension of 20×20 NF was used as both counter and reference electrode. Then the electrodeposition of Ni nanoparticles was carried out at a potential of -2 V using an AutoLab Potentiostat 302N (Metrohm, Holland) in a 20 mg mL^{-1} of NiCl_2 solution. The mass of the deposited nickel nanoparticles was controlled at ca. 1.9 mg cm^{-2} . After finishing the electrodeposition, the working electrode was taken out, rinsed with high purity of water and dried. The layered Ni/graphene/NF electrode (Ni/G/NF) was then obtained. Followed by activation of Ni/G/NF in KOH solution via cyclic voltammetry (CV) before electrochemical test, a layered

Ni(OH)₂/G composite was finally synthesized. A schematic synthesis route of the layered Ni(OH)₂/G composite is given in Figure 1.

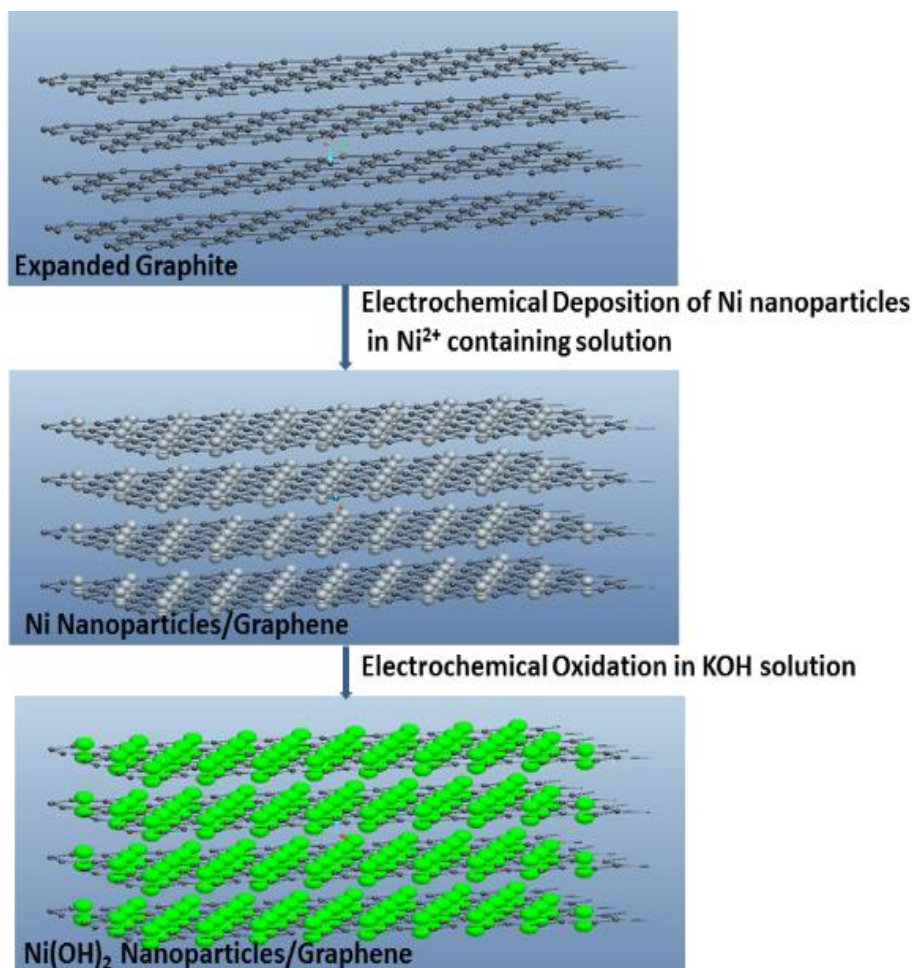


Figure 1. Schematic route for synthesis of layered Ni(OH)₂/G composite.

2.3 Characterization

Wide-angle (15-100°, 30 kV/20 mA) powder X-ray diffraction (XRD) was conducted using an X-ray diffractometer with Cu radiation at $\lambda=0.15406$ nm to measure the phases of the as-prepared composite. Zeiss EVO MA 15 scanning electron microscope (SEM) and transmission electron microscope (TEM, SAED, using Libra 200FE with an accelerating voltage of 200 kV) were applied to characterize the morphology and structure of the obtained Ni/G and Ni(OH)₂/G composites.

2.4 Electrochemical measurements

The electrochemical measurements were performed in a standard three-electrode cell by using an AutoLab Potentiostat 302N. The Ni/G/NF electrode was hot-pressed under 10 MPa for 1 min at

85 °C and then used as the working electrode. Hg/HgO and Pt coil were used as the reference electrode and the counter electrode, respectively.

Prior to electro-capacitive measurements, the deposited Ni nanoparticles on the Ni/G/NF electrode was converted into Ni(OH)₂ nanoparticles by cyclic voltammetry (CV) with a scan rate of 50 mV s⁻¹ in the potential range of 0.15-0.55 V. An activation procedure is usually conducted prior to an electrochemical measurement. Therefore, preparation of the layered Ni(OH)₂/graphene/NF electrode (Ni(OH)₂/G/NF) can be assumed as a one-step synthesis procedure from graphite, because the step of the deposited Ni nanoparticles converted to Ni(OH)₂ nanoparticles by CV can be considered as an electro-activation process rather than a step of composites synthesis. The specific capacitance was calculated from the CV curves using the following equation (1) and from discharging curves from equation (2):

$$C_s = \int IdV / mv\Delta V \quad (1)$$

where C_s represents the specific capacitance (F g⁻¹), I is the response current density (A cm⁻²), V is the potential (V), v is the potential scan rate (V s⁻¹), ΔV is the potential window (V), and m is the mass of the electroactive materials in the electrodes (g).

Meanwhile the electrochemical performance can also be investigated by galvanostatic charge-discharge (GCD) method in a three-electrode system. The specific capacitance can be written as:

$$C_s = I\Delta t / m\Delta V \quad (2)$$

where C_s represents the specific capacitance (F g⁻¹), I is the discharge current (A), Δt is the discharge time (s), ΔV is the potential window (V), and m is also the mass of the electroactive materials in the electrodes (g).

In addition, electrochemical impedance spectroscopy (EIS) was carried out at an open circuit potential and with a potential amplitude of 5 mV in a frequency range of 10⁵ Hz to 10⁻² Hz. Cycling stability is a crucial performance for an electrode material, thus the life-span test was carried out for 2000 cycles at a current density of 10 A g⁻¹.

3. RESULTS AND DISCUSSION

The XRD pattern of the Ni(OH)₂/G/NF electrode is shown in Figure 2. The diffraction peaks at 44.5°, 51.9°, 76.3°, 92.9° and 98.3° can be ascribed to (111), (200), (220), (311) and (222) crystalline facets of metallic nickel NF, respectively. There are no obviously characteristic peaks of Ni(OH)₂ to be observed, this is probably because the mass of Ni(OH)₂ (<3 mg cm⁻², 1.9 mg cm⁻² of the deposited Ni nanoparticles cannot totally be converted into Ni(OH)₂ due to passivation) is much less than that of the NF substrate (ca. 37~38 mg cm⁻²) and Ni(OH)₂ may mainly present in an amorphous state.[22, 23] Furthermore, the diffraction peak at 26.3° corresponding to (002) planes of EG is very weak. One of the reasons is similar as that of the above mentioned Ni(OH)₂ due to less mass of EG. Another reason could be that the Ni(OH)₂ nanoparticles inserted between EG layers and EG transformed into graphene. Graphene has no intensive peak at diffraction peak of 26.3°. The Ni(OH)₂/G/NF electrode was hot-pressed under 10 MPa for 1 min at 85°C, so it's almost impossible to separate Ni(OH)₂/G

composite from Ni foam, therefore Ni(OH)₂/G composite cannot be characterized by XRD directly. To confirm the above mentioned suggestion, 60 wt% Ni(OH)₂/XC-72 composite prepared by precipitation method, the Ni(OH)₂/XC-72/NF electrode was fabricated under identical conditions and characterized by XRD. No obvious peaks ascribed to Ni(OH)₂ were observed, but Ni(OH)₂/XC-72 powder was detected.[24]

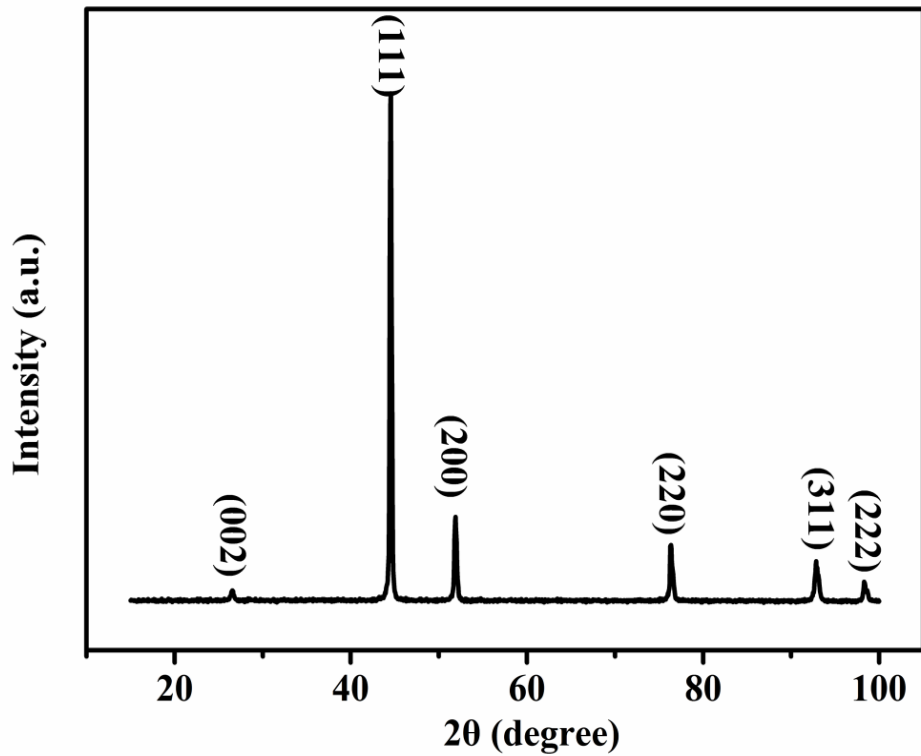
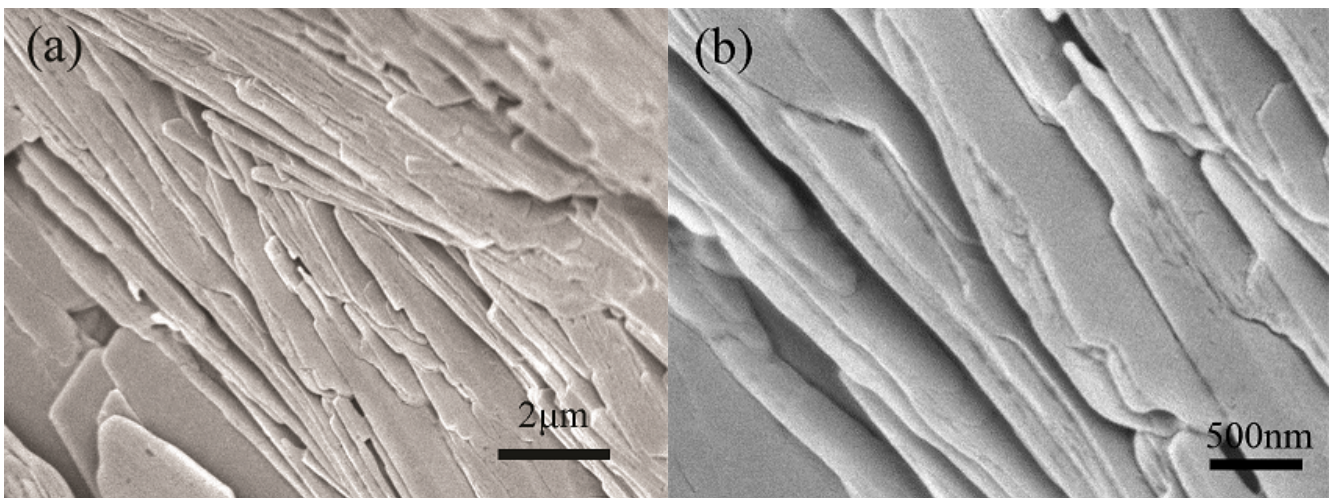


Figure 2. XRD pattern of Ni(OH)₂/G/NF electrode.



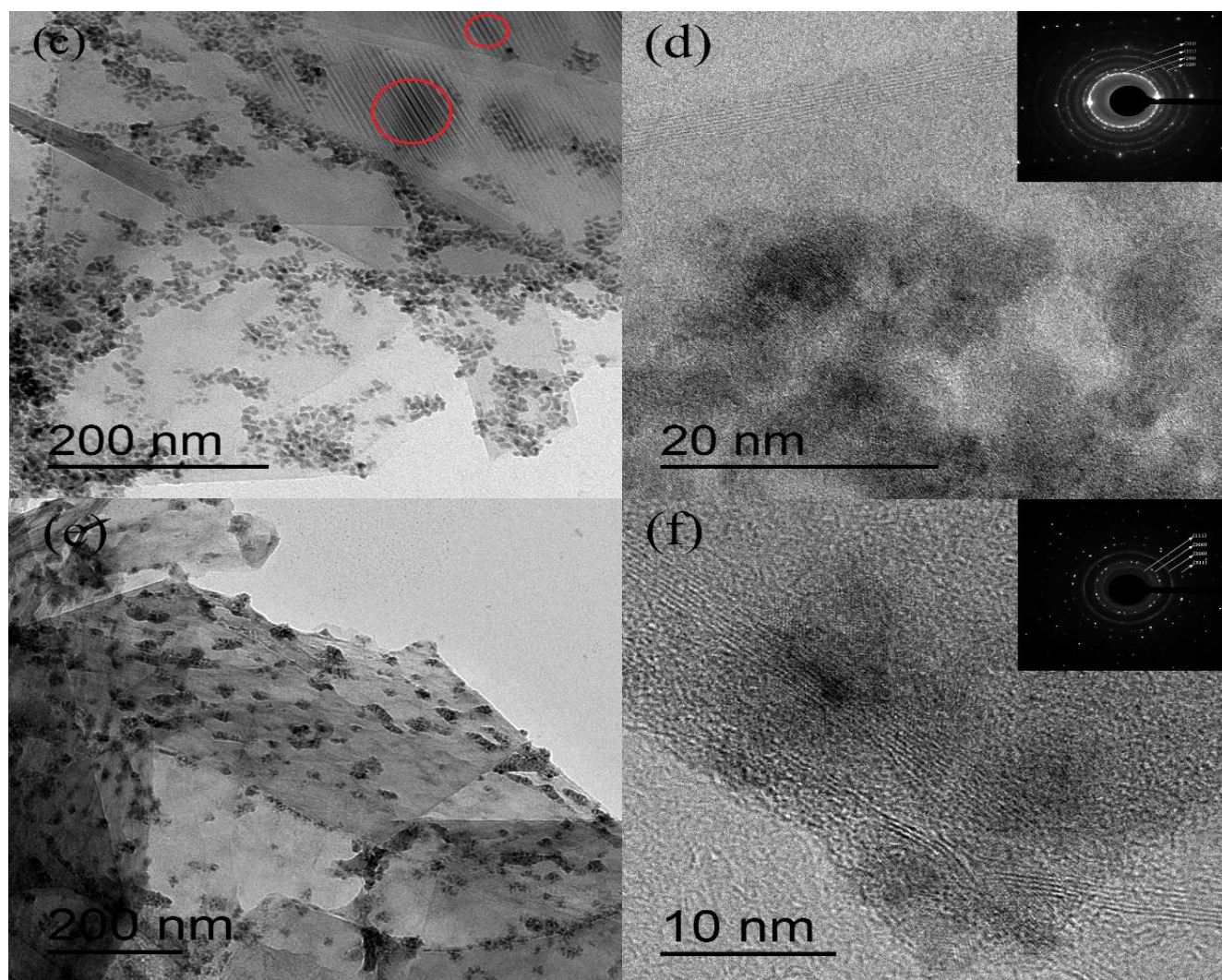


Figure 3. SEM images of EG (a, b) and TEM images of Ni/G (c, d) and Ni(OH)₂/G (e, f). Insets are SAED patterns of Ni/G (d) and Ni(OH)₂/G (f).

Fig. 3(a, b) show the FESEM images of EG. Expanded interlayer gaps can be observed, which makes it possible for Ni²⁺ entering the gaps and electrodeposited on the graphite in-planes. It is worth noting that the dimension of the graphite sheets is unchanged and thus EG can keep excellent electronic conductivity in-plane, which is essential for good rate capability of Ni(OH)₂/G composites. TEM images recorded the morphology of the layered Ni/G composite after electrodeposition, the results are shown in Fig. 3(c, d). The d-spacing of EG is calculated to be greater than 6 nm based on the region labeled by red circles from Fig. 3 (c), and EG contains less than 10 layers of graphite sheets which can be defined as graphene from Fig. 3 (d). [25] SEAD pattern of Ni/G as shown in the inset of Fig. 3 (d) confirms that the dark particles are metallic Ni particles. The diameter of primary Ni particles on Ni/graphene is in the range of several nanometers and uniformly deposited between graphene layers. After CV for 50 cycles between 0.15-0.55 V (*vs* Hg/HgO) in 6 M KOH before electrochemical tests, the layered Ni/G/NF electrode was activated and converted into a layered Ni(OH)₂/G/NF via the reaction $\text{Ni} + 2\text{OH}^- \rightarrow \text{Ni(OH)}_2 + 2\text{e}^-$. However, only part of the Ni

nanoparticles can be converted into $\text{Ni}(\text{OH})_2$ due to passivation phenomena of Ni metal. The TEM images of $\text{Ni}(\text{OH})_2/\text{G}$ are demonstrated in Fig. 3(e, f). The periodic diffraction rings from inside to outside in the SEAD pattern of $\text{Ni}(\text{OH})_2/\text{graphene}$ (in set of Fig. 3 (f)) can be indexed to the (111), (200), (220) and (311) plane of nickel oxide (JCPDF#47-1049) thanks to reaction of $\text{Ni}(\text{OH})_2 \rightarrow \text{NiO} + \text{H}_2\text{O}$ and side reaction of $\text{Ni} + 2\text{OH}^- \rightarrow \text{NiO} + \text{H}_2\text{O} + 2\text{e}^-$ that occurs during activation process when the electrode potential is more positive than 0.448 V theoretically. There are no diffraction rings belonging to $\text{Ni}(\text{OH})_2$ owing to its amorphous state which is in agreement with the result of XRD. The distribution and morphology of $\text{Ni}(\text{OH})_2$ nanoparticles are similar to those of pre-activated Ni nanoparticles. The $\text{Ni}(\text{OH})_2$ nanoparticles are small and uniformly distributed on graphene sheets, indicating that EG is a good carbon support.[26]

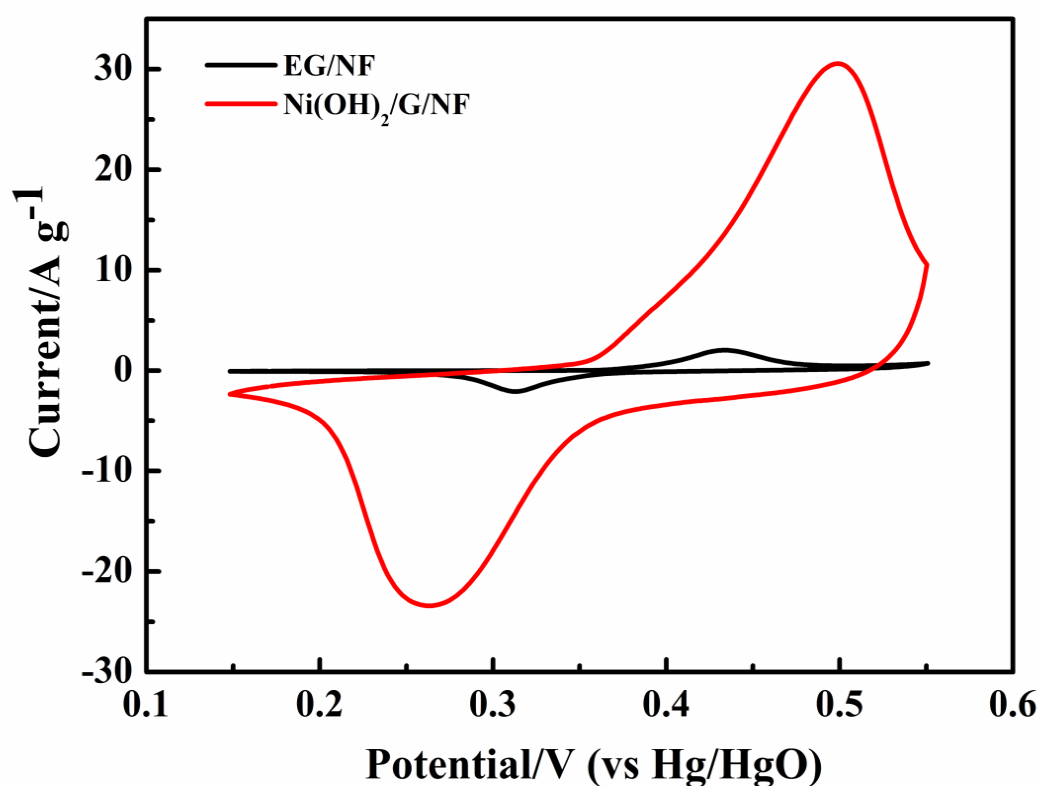


Figure 4. CV curves of EG/NF and $\text{Ni}(\text{OH})_2/\text{G}/\text{NF}$ at scan rate of 10 mV s^{-1} in 6 M KOH solution.

The electrochemical performances of the layered $\text{Ni}(\text{OH})_2/\text{G}$ for supercapacitors were tested using a three-electrode system in 6 M KOH aqueous solution. In general, cyclic voltammetry (CV) is considered as a convenient technique to characterize the capacitive behavior and quantify the capacitance of an electrode material by equation (1). Fig. 4 shows the CV curves of EG/NF and $\text{Ni}(\text{OH})_2/\text{G}/\text{NF}$ at a scan rate of 10 mV s^{-1} .

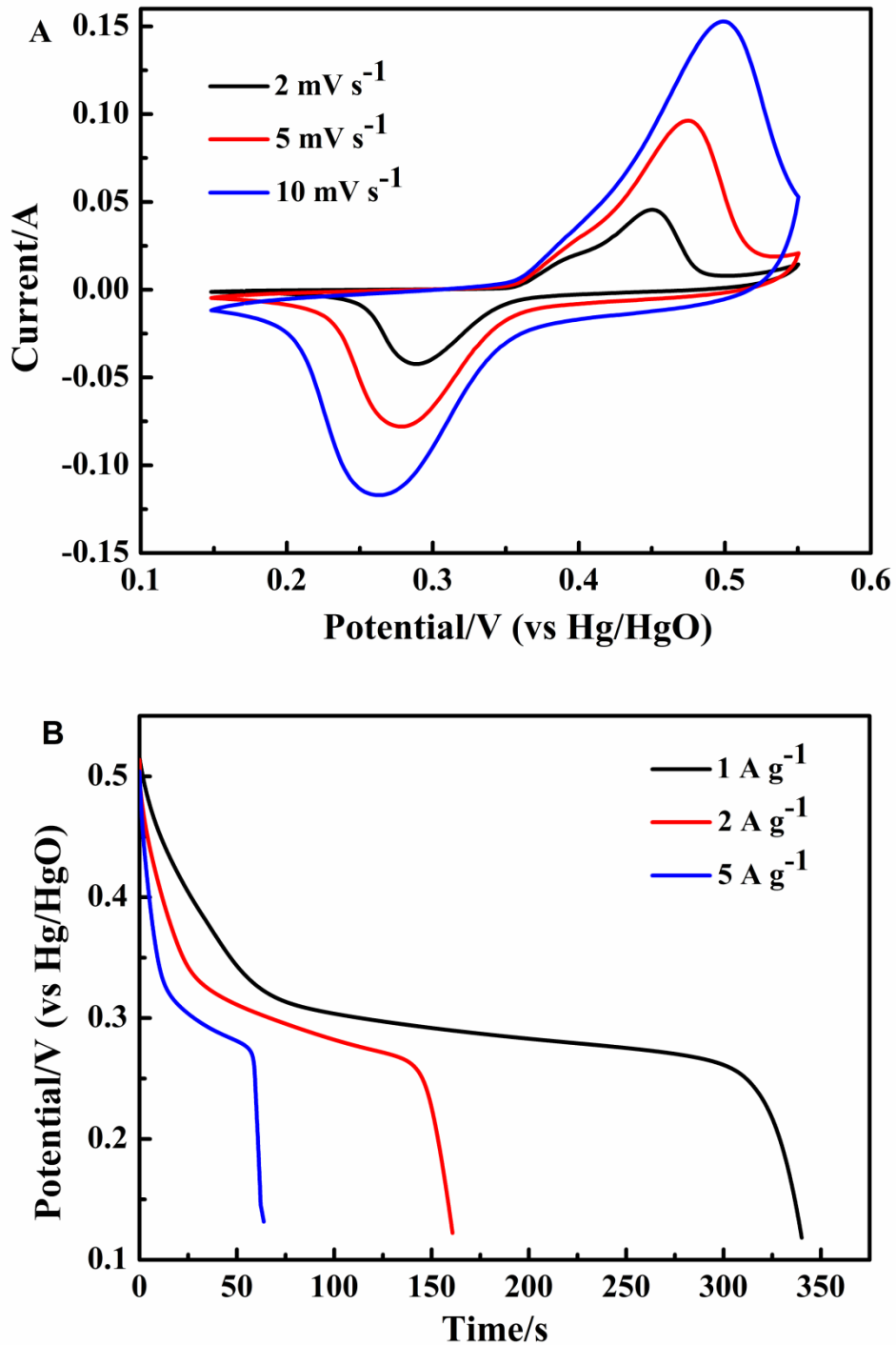
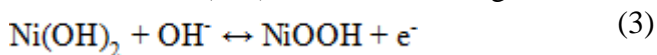


Figure 5. CV curves of Ni(OH)₂/G/NF at different scan rates (a) and discharging curves of Ni(OH)₂/G/NF at different current densities (b).

The peak current density of EG/NF is much smaller than Ni(OH)₂/G/NF, revealing that EG does not contribute much to the specific capacitance, and the specific capacitance of Ni(OH)₂/G/NF mainly comes from Ni(OH)₂ via the following redox reaction.[27]



From Fig. 5 (A), we can see that almost all of the CV curves exhibit a similar shape, and show an obvious pair of redox current peaks, indicating a typically pseudocapacitive behavior rather than an electric double layer capacitive characteristic. The specific capacitance at scan rate of 2 mV s^{-1} was calculated to be 815.6 F g^{-1} based on the active mass of materials coated on NF (ca. 5 mg cm^{-2}). When the scan rate increases from 2 mV s^{-1} to 5 mV s^{-1} and 10 mV s^{-1} , and the specific capacitance decreases from 815.6 F g^{-1} to 780.2 F g^{-1} and 733.6 F g^{-1} , respectively.

Galvanostatic charge and discharge (GCD) is a steady state method for measuring specific capacitances of electrode materials for ECs. Discharging curves of $\text{Ni(OH)}_2/\text{G}/\text{NF}$ at different current densities are given in Fig. 5 (B), all of them show a voltage plateau at about 0.3 V , suggesting a pseudocapacitive feature, which is consistent with the CV curves.[28] $\text{Ni(OH)}_2/\text{G}/\text{NF}$ demonstrates specific capacitances of 855.6 F g^{-1} , 810 F g^{-1} and 797.5 F g^{-1} at discharging current densities of 1 A g^{-1} , 2 A g^{-1} and 5 A g^{-1} . The specific capacitances and rate capabilities obtained from both CV and galvanostatic methods are listed in Table 1. The $\text{Ni(OH)}_2/\text{G}/\text{NF}$ electrode shows an excellent rate capability. For the CV method, as the scan rate increases from 2 mV s^{-1} to 10 mV s^{-1} , the specific capacitance decreased by 10%; as for galvanostatic discharging, from discharging current increases from 1 to 5 A g^{-1} , the specific capacitance only decreases by 7%. The rate capability measured by galvanostatic discharging is better than that by CV, because the former is a steady test technique and the latter is a transient test technique. Correlating the SEM image of $\text{Ni(OH)}_2/\text{G}/\text{NF}$, Ni(OH)_2 nanoparticles with an average particle size of ca.6nm, results in a relatively fast faradaic reaction.

Table 1. The specific capacitances and rate capabilities of $\text{Ni(OH)}_2/\text{G}/\text{NF}$ obtained from CV and galvanostatic methods.

CV			Galvanostatic		
v (mV s^{-1})	C_s (F g^{-1})	Rate capability	I (A g^{-1})	C_s (F g^{-1})	Rate capability
2	815.6	100 %	1	855.6	100 %
5	780.2	96 %	2	810	95%
10	733.6	90 %	5	797.5	93%

The specific capacitance of $\text{Ni(OH)}_2/\text{G}/\text{NF}$ is also compared with the reported literature data of $\text{Ni(OH)}_2/\text{rGO}$ prepared by various methods, as shown in Table 2. The specific capacitance of $\text{Ni(OH)}_2/\text{G}/\text{NF}$ is comparable to the reported data even though much larger areal loading was used in our work.[9,17,19-21,29-32] Furthermore, we only spent several minutes more to complete preparation of electrode materials and fabrication of electrodes than a conventional procedure to fabricate electrodes, and our used EG is considerably cheaper than rGO, the procedure is simple, controllable, easily handled and scaled-up.

Table 2. Comparison of specific capacitances of Ni(OH)₂/G composites prepared by various methods.

Materials	Preparation Method	Current density (A g ⁻¹)	C _s (F g ⁻¹)	Ref.
α-Ni(OH) ₂ /rGO	Chemical precipitation	1	1672	9
β-Ni(OH) ₂ /rGO	Hydrothermal process	1	1875	29
Ni(OH) ₂ -rGO	Hydrothermal process	1	1795	30
Ni(OH) ₂ /rGO	Electrophoretic deposition	2	1404	31
Ni(OH) ₂ /rGO	Solvothermal process	2.7	1552	32
Ni(OH) ₂ /G/NF	Electrodeposition	3	2161	20
RGO/Ni(OH) ₂ /NF	Hydrothermal process	3.3	1667	19
β-Ni(OH) ₂ /rGO	Electrodeposition	5	1700	21
rGO&Ni(OH) ₂	Chemical precipitation	6	1576	17
Ni(OH) ₂ /G/NF	Electrodeposition	1	900	33
Ni(OH) ₂ /G	Solvothermal process	0.2	959.9	34
Ni(OH) ₂ /G/NF	Electrodeposition	1	856	This Work

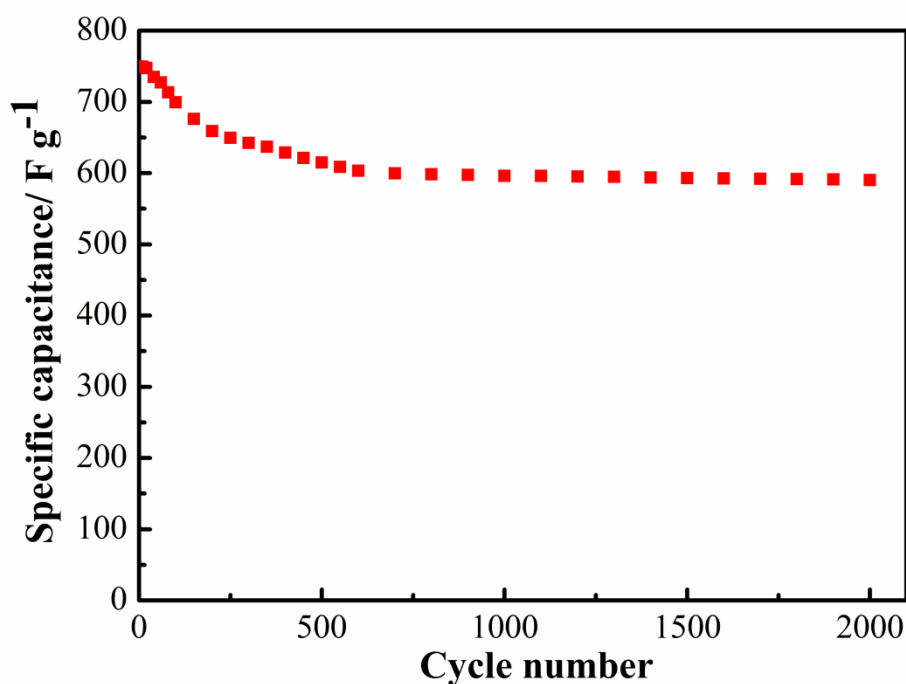
**Figure 6.** Cycling stability of Ni(OH)₂/G/NF electrode at current density of 10 A g⁻¹.

Fig. 6 illustrates the cycling stability of Ni(OH)₂/G/NF electrode at 10 A g⁻¹. The specific capacitance decreases from 749.5 F g⁻¹ to 599.6 F g⁻¹ after about 700 cycles, then almost maintaining a constant value with specific capacitance retention of 80.8%. An obvious decrease of specific capacitance during the initial 700 charge-discharge cycles is observed. From 700th to the 2000th cycle, the Ni(OH)₂/G/NF electrode shows an excellent cycling stability. Three reasons can be attributed to

this excellent cycling stability, one is that graphite-like dimensions of graphene sheets can make the Ni(OH)₂/G/NF keep good electron conductivity because of excellent conductivity in-plane of graphite sheets; secondly, we can see that the Ni(OH)₂ nanoparticles are anchored on the planes and the brinks of graphene sheets, which make them difficult to move and aggregate; and furthermore the layered nanostructure also helps to maintain the specific capacitance quite well. These can be further confirmed by electrochemical impedance spectroscopy (EIS).

The EIS Nyquist plots of Ni(OH)₂/G/NF was recorded at frequency ranging from 0.01 Hz to 10⁵ Hz at open circuit potential in 6 M KOH solution, as shown in Fig. 7. The equivalent series resistance (ESR) before and after 2000 cycles obtained from the X-axis intercept of the inset plot is 0.4 Ω and 0.39 Ω. For a three-electrode system, this ESR is very small, which means that the Ni(OH)₂/G/NF electrode has a good electronic conductivity, and indicates that the demerits of poor electrical conductivity of Ni(OH)₂ is overcome by incorporating of EG, because EG has excellent in-plane conductivity. A bit descending ESR value of Ni(OH)₂/G/NF is due to the exfoliation of poorly conductive materials of Ni(OH)₂ from the electrode. This is consistent with the cycling stability result. According to EIS principle, a smaller semicircle means a lower charge-transfer resistance, and a higher slope means a lower diffusion resistance.[35]

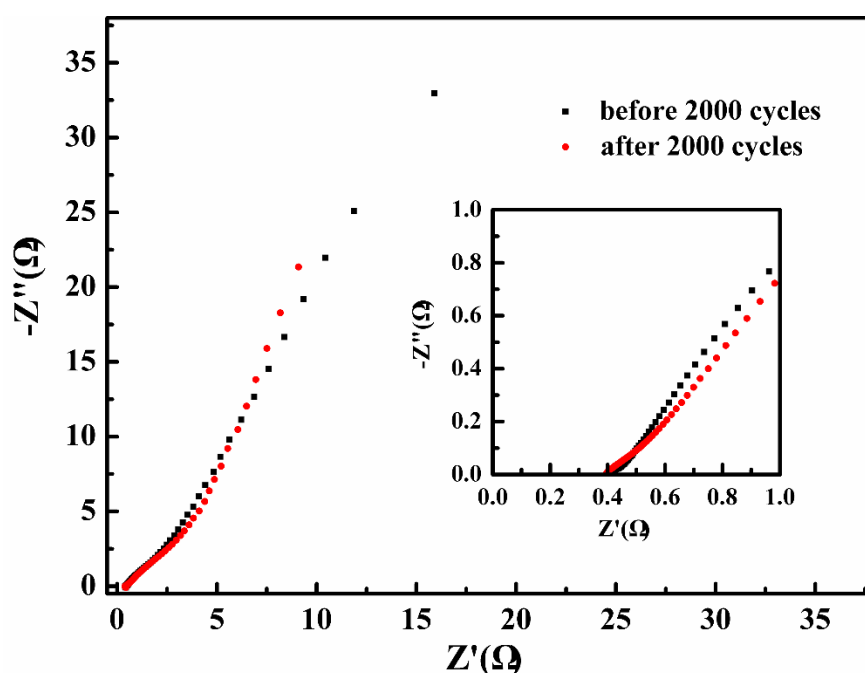


Figure 7. EIS Nyquist plot of Ni(OH)₂/G/NF electrode at open circuit potential.

From Fig. 7, it can also be observed that the diameter of the semicircle of Ni(OH)₂/G/NF is small and the slope of the straight line in the low frequency region is more close to $-Z''$ axis, which indicate that the Ni(OH)₂/G/NF electrode has low charge transfer resistance and small ion diffusion resistance. In other words, during charging and discharging process, the redox reaction of Ni(OH)₂ can occur easily because it belongs to pseudocapacitive reactions, without new compounds formed such as in battery reactions. A layered nanostructure facilitates ions diffusion and leads to small mass transportation resistance. It can be concluded that Ni(OH)₂/G/NF has excellent cycle stability

according to the EIS test result, the Nyquist plots of Ni(OH)₂/G/NF are nearly unchanged after 2000 cycles.

4. CONCLUSIONS

This work provides an approach of fabrication of Ni(OH)₂/G/NF electrode by electrochemical deposition of nickel nanoparticles on expanded graphite sheets, followed by converting nickel nanoparticles into Ni(OH)₂ or NiO nanoparticles during the conventional activation process. The procedure is environmentally friendly, and time-saving. The electrode demonstrates an excellent specific capacitance and cycling stability, and the as-prepared Ni(OH)₂/G/NF electrode is quite cost effective. The technique is easily scaled up and expected to solve the big issues of high cost and low energy density that supercapacitors confront.

ACKNOWLEDGEMENTS

This work was supported by International Technology Collaboration of Chengdu Science and Technology Division, Scientific Research Foundation for Returned Scholars, Ministry of Education of China, the Open Project from State Key Lab of Catalysis(N-14-1), the Technology Project of Education Department of Sichuan Province (13ZA0193), Youth Science and Technology Innovation Team of Electrochemistry for Energy Materials, Southwest Petroleum University (2015CXTD04).

References

1. P. Simon and Y. Gogotsi, *Nat. Mater.*, 7 (2008) 845.
2. H. Talbi, P.E. Just and L.H. Dao, *J. Appl. Electrochem.*, 33 (2003) 465.
3. G.W. Yang, C.L. Xu and H.L. Li, *Chem. Comm.*, 48 (2008) 6537.
4. B. Wang, J.S. Chen, Z.Y. Wang, S. Madhavi and X.W. Lou, *Adv. Energy Mater.*, 2 (2012) 1188.
5. L.D. Feng, Y.F. Zhu, H.Y. Ding and C.Y. Ni, *J. Power Sources*, 267 (2014) 430.
6. J. Xu, X.F. Gu, J.Y. Cao, W.C. Wang and Z.D. Chen, *J. Solid State Electr.*, 16 (2012) 2667.
7. J. Xu, L. Li, F. He, R.C. Lv and P.P. Yang, *Electrochim. Acta*, 148 (2014) 211.
8. J.T. Zhang, S. Liu, G.L. Pan, G.R. Li and X.P. Gao, *J. Mater. Chem. A*, 2 (2014) 1524.
9. S. Bag and C.R. Raj, *J. Mater. Chem. A*, 2 (2014) 17848.
10. X.W. Ma, J.W. Liu, C.Y. Liang, X.W. Gong and R.C. Che, *J. Mater. Chem. A*, 2 (2014) 12692.
11. G.S. Gund, D.P. Dubal, S.S. Shinde and C.D. Lokhande, *ACS Appl. Mater. Interfaces*, 6 (2014) 3176.
12. L.P. Sui, S.H. Tang, Y.D. Chen, Z. Dai, H.X. Huangfu, Z.T. Zhu, X.L. Qin, Y.X. Deng, G.M. Haarberg, *Electrochim. Acta*, 182 (2015) 1159.
13. H.D. Liu, J.L. Zhang, B. Zhang, L. Shi, S.Z. Tan and L.H. Huang, *Electrochim. Acta*, 138 (2014) 69.
14. J.C. Huang, P.P. Xu, D.X. Cao, X.B. Zhou, S.N. Yang, Y.J. Li and G.L. Wang, *J. Power Sources*, 246 (2014) 371.
15. J.L. Xia, F. Chen, J.H. Li and N.J. Tao, *Nat. Nanotech.*, 4 (2009) 505.
16. S. Park and R.S. Ruoff, *Nat. Nanotech.*, 4 (2009) 217.
17. J.L. Zhang, H.D. Liu, L.H. Huang, S.Z. Tan, W.J. Mai and X. Cai, *J. Solid State Electr.*, 19 (2014) 229.
18. D.P. Dubal, R. Holze and P. Gomez-Romero, *Sci. Rep.*, 4 (2014) 7349.

19. S.D. Min, C.J. Zhao, G.R. Chen, Z.M. Zhang and X.Z. Qian, *Electrochim. Acta*, 115 (2014) 155.
20. L.Q. Wang, X.C. Li, T.M. Guo, X.B. Yan and B.K. Tay, *Int. J. Hydrogen Energ.*, 39 (2014) 7876.
21. Z.X. Yang, C.H. Fang, Y. Fang, Y.Q. Zhou and F.Y. Zhu, *Int. J. Electrochem. Sci.*, 10 (2015) 1574.
22. S.L. Gong, Q. Cao, L.E. Jin, C.G. Zhong and X.H. Zhang, *J. Solid State Electrochem.*, 20 (2016) 619.
23. Y.Y. He, J.J. Zhang and J.W. Zhao, *Acta Phys. -Chim. Sin.* 30 (2014) 297.
24. S.H. Tang, L.P. Sui, Z. Dai and H.X. Huangfu, *RSC Adv.*, 5 (2015) 43164.
25. T. Wang, S.L. Zhang, X.B. Yan, M.Q. Lyu, L.Z. Wang, J. Bell and H.X. Wang, *ACS Appl. Mater. Interfaces*, 9 (2017) 15510.
26. I.M. Afanasov, O.N. Shornikova, V.V. Avdeev, O.I. Lebedev, G. Van Tendeloo and A.T. Matveev, *Carbon*, 47 (2009) 513.
27. C.-C. Hu, K.-H. Chang and T.-Y. Hsu, *J. Electrochem. Soc.*, 155 (2008) F196.
28. J. Tizfahm, B. Safibonab, M. Aghazadeh, A. Majdabadi, B. Sabour and S. Dalvand, *Colloids and Surfaces A: Physicochem. Eng. Aspects*, 443 (2014) 544.
29. W. Liu, C. Ju, D. Jiang, L. Xu, H.P. Mao and K. Wang, *Electrochim. Acta*, 143 (2014) 135.
30. U. Singh, A. Banerjee, D. Mhamane, D. Mhamane, A. Suryawanshi, K.K. Upadhyay and S. Ogale, *RSC Adv.*, 4 (2014) 385.
31. H.T. Zhang, X. Zhang, D.C. Zhang, X.Z. Sun, H. Lin, C.H. Wang and Y.W. Ma, *J. Phys Chem B*, 117 (2013) 1616.
32. Y. Wang, S.L. Gai, N. Niu, F. He and P.P. Yang, *J. Mater. Chem. A*, 1 (2013) 9083.
33. S. Ruiz-Gomez, A. Bosca, L. Perez, J. Pedros, J. Martinez, A. Paez and F. Calle, *Diam. Relat. Mater.*, 57 (2015) 63.
34. Y.F. Liu, G.H. Yuan, Z.H. Jiang, Z.P. Yao and M. Yue, *J. Alloy. Compd.*, 618 (2015) 37.
35. R.D. Armstrong and H. Wang, *Electrochim. Acta*, 36 (1991) 759.